Oil & Gas Science and Technology - Rev. IFP Energies nouvelles **73**, 40 (2018)

https://doi.org/10.2516/ogst/2018046

Available online at:
www.ogst.ifpenergiesnouvelles.fr

REGULAR ARTICLE OPEN ACCESS

Heat conduction and thermal convection on thermal front movement during natural gas hydrate thermal stimulation exploitation

Yongmao Hao[1,*], Xiaozhou Li[1,*], Shuxia Li[1], Guangzhong Lü[2], Yunye Liu[1], and Xinlin Wei[1]

[1] College of Petroleum Engineering, China University of Petroleum, Qingdao, Shandong 266580, China
[2] Research Institute of Petroleum Exploration and Development, Shengli Oilfield Company, Sinopec, Dongying 257015, China

Received: 19 March 2018 / Accepted: 24 July 2018

Abstract. Natural Gas Hydrate (NGH) has attracted increasing attention for its great potential as clean energy in the future. The main heat transfer mode that controls the thermal front movement in the process of NGH exploitation by heat injection was discussed through NGH thermal stimulation experiments, and whether it is reliable that most analytical models only consider the heat conduction but neglect the effect of thermal convection was determined by the comparison results between experiments and Selim's thermal model. And the following findings were obtained. First, the movement rate of thermal front increases with the rise of hot water injection rate but changes little with the rise of the temperature of the injected hot water, which indicated that thermal convection is the key factor promoting the movement of thermal front. Second, the thermal front movement rates measured in the experiments are about 10 times that by the Selim's thermal model, the reason for which is that the Selim's thermal model only takes the heat conduction into account. And third, theoretical calculation shows that heat flux transferred by thermal convection is 15.56 times that by heat conduction. It is concluded that thermal convection is the main heat transfer mode that controls the thermal front movement in the process of NGH thermal stimulation, and its influence should never be neglected in those analytical models.

Nomenclature

v	The movement rate of the thermal front (cm/min)
r	The position of measuring point (cm)
t	Time (min)
T	Temperature (°C)
u	The flow velocity of fluid (m/s)
x	Location along the porous medium (m)
φ	Porosity dimensionless
ρ	Density (g/m^2)
C	Heat capacity (kJ/(kg K))
λ	Thermal conductivity (W/(m K))
Q	Heat flux transferred by convection heat transfer (W)
Q_1	Heat flux transferred by heat conduction (W)
Q_2	Heat flux transferred by thermal convection (W)
h	Convective heat transfer coefficient (W/(m^2 K))
A	Surface area (m^2)
δ	Thickness (m)
t_f	Temperature of the hot water (°C)
t_w	Temperature of initial NGH reservoir (°C)

* Corresponding authors: upc_lixiaozhou@163.com; haoyongmao@163.com

1 Introduction

Natural Gas Hydrate (NGH) is regarded as the most promising alternative energy resource because of its wide distribution, large resources and cleanliness [1–4]. There exist three basic techniques to extract gas contained within NGH sediment, which are thermal stimulation, depressurization and chemical inhibitor stimulation [5–7]. Thermal stimulation is believed to be the one of most effective of the three methods, and the movement of thermal front is the key factor controlling the exploitation procedure [8–10]. Many simulation studies have been performed for the exploitation of NGH from hydrate reservoirs through thermal injection. Regarding the hydrate dissociation as a moving boundary ablation process, Selim and Sloan [11] established an analytical hydrate dissociation model under thermal stimulation, concluding that the thermal front is a constant temperature boundary moving at a rate proportional to $t^{-1/2}$. Tang *et al.* [12] developed a thermodynamic mathematical model of hydrate dissociation to obtain temperature distribution of the dissociated zone and hydrate zone, and the hydrate decomposition heat to total heat input ratio had also been analyzed based on this model. Based on the Selim's thermal model, Li *et al.* [13] considering

the initial hydrate saturation, developed a one-dimensional mathematical model of hydrate dissociation. They concluded that the thermal dissociation front of NGH is mainly influenced by porosity, injection temperature, initial hydrate saturation, initial hydrate temperature, thermal conductivity and thermal diffusivity of the dissociated zone. Li *et al.* [14] presented a mathematical model for radial, quasi-steady state heat transfer considering the Stefan moving boundary problem. The temperature distribution and the dissociation frontal brim location were determined in this model. All of the above analytical models only consider the heat transfer mode of heat conduction but ignore the effect of thermal convection in the process of NGH heat injection. However, many studies of thermal recovery in traditional reservoirs indicate that heat conduction and thermal convection are both important heat transfer methods in porous media [15–18]. Therefore, the reliability of the method ignoring thermal convection in most analytical models of NGH thermal stimulation remains controversial. While the heat transfer is an important property used to model the NGH decomposition process, few studies have focused on the effects of heat transfer mode [19–21]. In this study, we carried out NGH thermal stimulation experiments by focusing on the main heat transfer mode that controls the thermal front movement in the process of NGH exploitation by thermal stimulation. And then, the NGH thermal stimulation experiment results were compared with the Selim's thermal model to verify the reliability of the method of neglecting thermal convection in analytical models.

2 Experiment

2.1 Experimental materials and methods

A schematic of the experimental apparatus used in this work is shown in Figure 1. The NGH synthesis and exploitation experimental simulation system includes air feed module, feed flow module, synthesis and exploitation module, environmental simulation module, back pressure control module, metering module, data acquisition and process module [22]. The air feed module is mainly used for the NGH synthesis process, which is responsible for providing stable pressure and methane to the synthesis and exploitation module, and the feed flow module is charge of injecting water or chemistry into the synthesis and exploitation module. The synthesis and exploitation module is the core component of experimental simulation system, NGH is synthesized and dissociated in this module. The environmental temperature and outlet pressure will be controlled by environmental simulation and back pressure control module, respectively. The experimental data will be automatically and timely collected by the metering module and the data acquisition and process module.

The experimental model is one-dimensional sand filling tube, whose size is Φ25 mm × 500 mm. There are four temperature sensors evenly arranged along the line, which represent the four measuring points, and the positions of the four measuring points are 0 cm, 12.5 cm, 25.0 cm, 37.5 cm and 50.0 cm. After filling sand, the permeability and the porosity of this experimental model are 1.11 μm^2 and 32.8%. The water used in this experiment is salt water with 2% mass percentage concentration and the gas used in this experiment is CH_4 with the purity of 99.9%. Experimental procedures are as follows: (1) NGH isovolumetric formation: First, inject methane and water into the porous medium tube with a constant rate to the scheduled pressure 8–10 MPa. Then, close the inlet and outlet valves and then keep the temperature of the thermostat at 1.0 °C for methane hydrate formation. When the pressure in the tube does not decline anymore, the NGH formation process is considered to be completed. (2) NGH dissociation by thermal stimulation: set the temperature of preheat vessel at a certain value to heat the water, when it is steady, inject hot water into the porous medium tube at a constant rate. NGH continuously dissociated since the heat transfers from the boundaries to the NGH reservoir. The temperature changes at each measuring point are recorded during the NGH thermal stimulation experiment [22–24].

2.2 Analysis of the experimental results

When it comes to NGH exploitation by thermal stimulation, the dissociation of NGH is a process of continuous advancing of the thermal front, and the NGH reservoir is divided by the thermal front into dissociation zone and hydrate zone. NGH dissociates at thermal front between the dissociation and hydrate zone only. The NGH dissociation temperature is 3 °C in the experiment, where the temperature reaches the NGH dissociation temperature is defined as the thermal front [25, 26]. The heat exchanges during the NGH thermal stimulation experiment are mainly including follow aspects: (1) heat exchanging with the porous medium of NGH reservoir; (2) the latent heat because of NGH dissociate at the thermal front; (3) heat exchanging with the dissociated gas and water resulting from the NGH dissociation process. In order to reduce heat loss of tube, specialized heat preservation sponge tube was used, which can wrap up heat injection tube and sand filling tube tightly. Therefore, the heat lost exchanging with external environment is less and can be ignored in this experiment. Two kinds of NGH thermal stimulation experiments were performed in this paper, constant water injection rate experiment (test 1–4) and constant water injection temperature experiment (test 5–8). The basic date is shown in Table 1.

2.2.1 NGH thermal stimulation experiment at constant injection rate

In the NGH thermal stimulation experiment at constant injection rate, the water was injected at a constant rate of 0.97 cm/min, and the water injection temperatures were set at 42 °C, 62 °C, 78 °C and 84 °C for tests 1–4 NGH exploitation experiments. Take the water injection temperature of 78 °C as an example. Figure 2 shows the temperature over time curve of the four measuring points at constant injection rate. It can be seen that there is an apparent increase in the temperature of each measuring point at the beginning, and then the increase slows, and finally stable at a certain level. This is because the reservoir

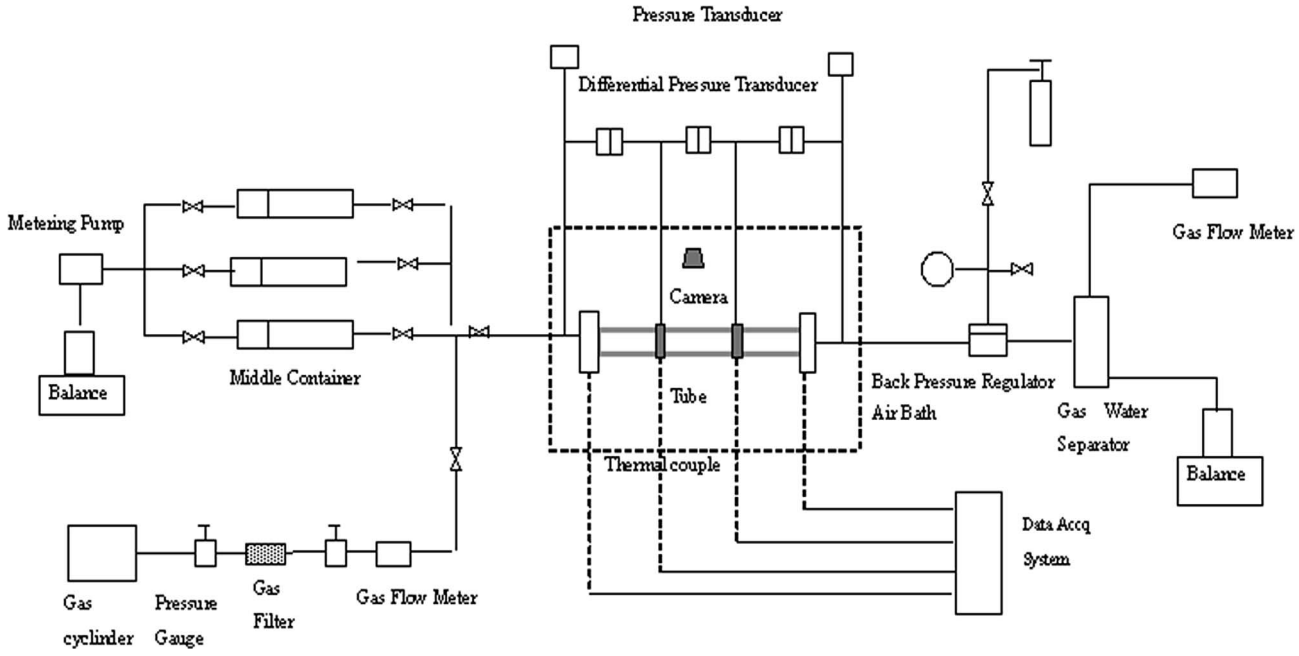

Fig. 1. NGH synthesis and exploitation experiment simulation system flow diagram.

Table 1. Basic data of NGH exploitation by thermal stimulation experiment.

Test number	Parameters			
	Initial temperature (°C)	Initial pressure (MPa)	Water injection rate (cm/min)	Water injection Temperature (°C)
1	1	3.4	0.97	42
2	1	3.4	0.97	62
3	1	3.4	0.97	78
4	1	3.4	0.97	84
5	1	3.4	0.97	78
6	1	3.4	0.70	78
7	1	3.4	0.44	78
8	1	3.4	0.22	78

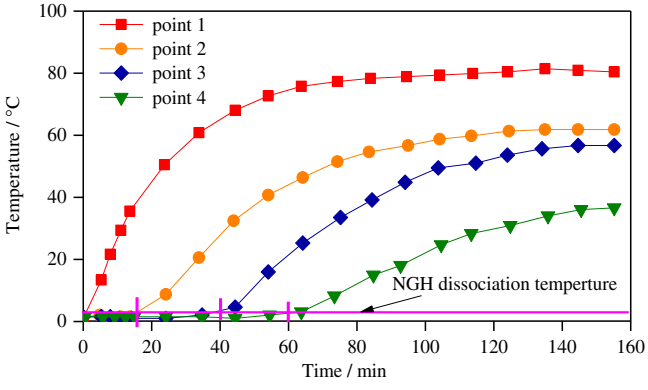

Fig. 2. Distribution of temperature under different measuring points *vs.* time.

temperature is 1 °C before the hot water is injected, once the reservoir is heated by the hot water at a certain place, the temperature there will increase rapidly. Additionally, as the increase of time, the heat exchanging between the hot water and porous medium increase. To some extent, the heat exchanging among the hot water, gas and porous medium comes to the dynamic balance heat transfer, then the temperature of the each measuring point will remain at a steady value. The temperature of each measuring point increases in turn, and it is obvious that the thermal front is advancing forward with time. The thermal front reaches the measuring point 2, 3 and 4 at the time of 18 min, 40 min and 60 min respectively, thus the movement rate of the thermal front could be calculated as follows:

$$v = \frac{r}{t}. \quad (1)$$

In Figure 3a, hot water at temperature of 42 °C, 62 °C, 78 °C and 84 °C was injected at a constant rate 0.97 cm/min. It can be observed that the movement rate of thermal front increases slightly with the increase of the injected water temperature. Figure 3b shows the average thermal front movement rate curve at different injection water temperatures. The average thermal front movement rates are 0.78 cm/min, 0.86 cm/min, 0.94 cm/min, 0.98 cm/min for hot water injection temperatures of 42 °C, 62 °C, 78 °C and 84 °C, respectively. When the

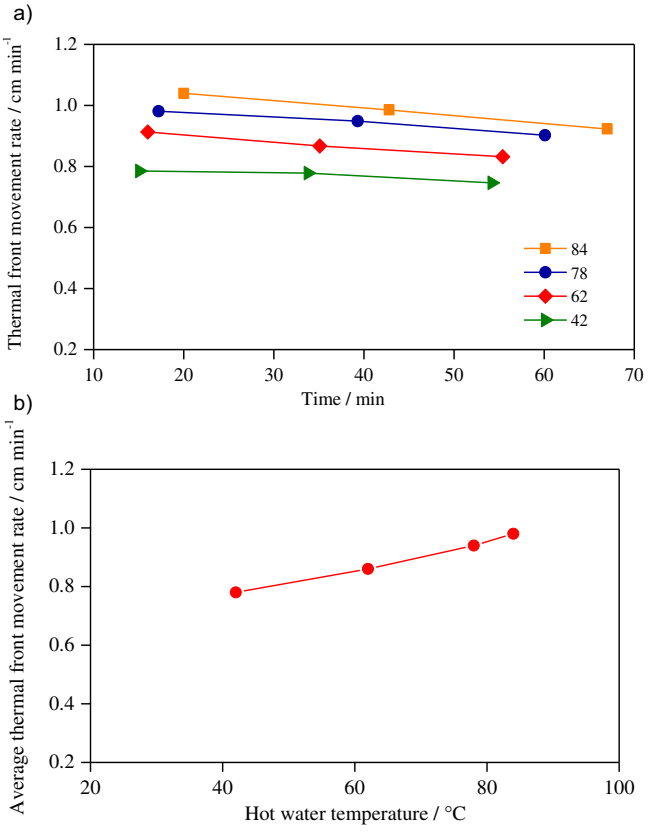

Fig. 3. (a) Thermal front movement rate under different hot water temperature vs. time. (b) Average thermal front movement rate under different hot water temperature.

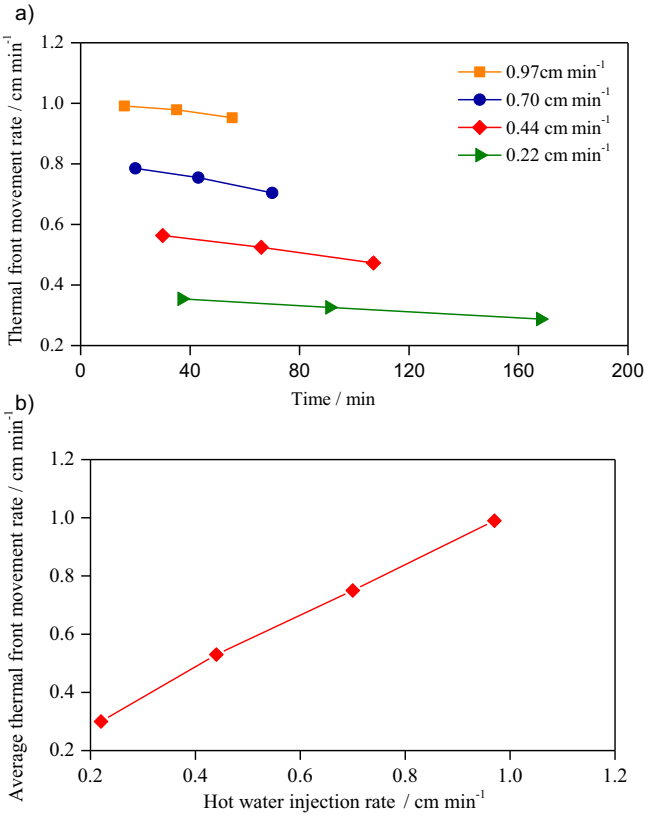

Fig. 4. (a) Thermal front movement rate under different hot water injection rate vs. time. (b) Average thermal front movement rate under different hot water injection rate.

hot water injection temperature is increased 1 time (rise from 42 °C to 84 °C), the average thermal front movement rates increased only by 25.6% (rise from 0.78 cm/min to 0.98 cm/min). Therefore, the hot water injection temperature has little impact on the movement rate of thermal front, which indicates that the heat conduction is not the main heat transfer mode that controls the thermal front movement in the process of NGH exploitation by heat injection.

2.2.2 NGH thermal stimulation experiment at constant temperature of injection water

In order to further verify the main heat transfer mode that controls the thermal front movement in the process of NGH exploitation by thermal stimulation, the temperature of injection hot water was kept constant at 78 °C, and the water injection rates were set at 0.97 cm/min, 0.70 cm/min, 0.44 cm/min and 0.22 cm/min for tests 5–8 NGH exploitation experiments, respectively. The thermal front movement rate curves were shown in Figure 4a. It can be seen that the thermal front movement rate increases with the increase of the hot water injection rate. Additionally, under the conditions of constant hot water temperature and injection rate, the movement rate of thermal front decreases with a longer dissociation time due to more heat loss in the reservoir.

Figure 4b shows the average thermal front movement nearly increases linearly with the increase of hot water injection rate at a constant hot water temperature of 78 °C. The average thermal front movement rates are 0.30 cm/min, 0.53 cm/min, 0.75 cm/min and 0.99 cm/min for hot water injection rates of 0.22 cm/min, 0.44 cm/min, 0.70 cm/min and 0.97 cm/min, respectively. When the hot water injection rate increased 1 time (rise from 0.22 cm/min to 0.44 cm/min), the average thermal front movement rate has increased by 77% (rise from 0.31 cm/min to 0.53 cm/min). When the hot water injection rate increased 1.2 times (rise from 0.44 cm/min to 0.97 cm/min), the average thermal front movement rate has increased by 87% (rise from 0.53 cm/min to 0.99 cm/min). In comparison with the NGH thermal stimulation experiment at constant injection rate we mentioned above, we can come to the conclusion that the movement of thermal front is mainly determined by the hot water injection rate rather than hot water injection temperature, that is to say, the thermal convection is the main heat transfer mode promoting the thermal front movement in the process of NGH thermal stimulation.

3 Comparison with Selim's Thermal Model

The NGH thermal stimulation experiment results show that the movement rate of thermal front is mainly

promoted by the thermal convection, while the heat conduction has little effect on it. The energy balance equations for the NGH dissociation in the process of NGH thermal stimulation can be written as follows [27]:

$$\lambda_s \frac{\partial^2 T}{\partial x^2} + \frac{\partial T}{\partial x}(\rho_l C_l u_l) - e_H = (\mathrm{C}\rho)_s \frac{\partial T}{\partial t}, \qquad (2)$$

where $(\mathrm{C}\rho)_s = \phi\rho_{l+H}C_{l+H} + (1-\phi)\rho_R C_R$, $\lambda_s = \phi\lambda_{l+H} + (1-\phi)\lambda_R$, the subscripts l, H and R identify the fluid, NGH and rock. According to equation (2), the first term represents the thermal convection, the second term represents the heat conduction and the third term represents the latent heat caused by NGH dissociate. However, the literature survey shows there are many NHG thermal injection analytical models which consider the only transfer mode of heat conduction, ignoring the transfer mode of thermal convection. In these analytic models, the Selim's thermal model is the most typical and has the most application and greatest impact. To verify the reliability of these models, this paper compares the NGH thermal stimulation experiment results with the Selim's thermal model.

Selim's thermal model regards a uniform distribution of NGH in the porous medium. Initially, the hydrates are assumed to fill the entire porosity φ, and the initial temperature T_i, occupies the semi-infinite area $0 < x < \infty$. At time $t = 0$, the temperature at the boundary $x = 0$ is raised to T_0, which is higher than NGH dissociation temperature, the hydrates begin to dissociate. As a result, the thermal front separates the NGH reservoirs as two zones, zone I is dissociation zone occupies the area $0 < x < x(t)$, zone II is hydrates zone occupies the area $x(t) < x < \infty$. It is worth emphasizing that Selim neglects the thermal convection term in the process of solving the thermal model. The establishment and treatment were described in details by Selim and Sloan [11].

In this work, the basic parameters of NGH reservoir used in the Selim's thermal model are consistent with the NGH thermal stimulation experiment, which is shown in Table 2.

With the basic parameters shown in Table 2, inlet temperature T_0 was set at 42 °C, 62 °C and 78 °C, at the time of 60 min, the temperature distribution for the Selim's thermal model and NGH thermal stimulation experiment were calculated and are presented in Figure 5.

(1) Analysis of the temperature profile for Selim's thermal model, as we can see in Figure 5, the thermal front reached at particular distances of 3 cm, 5 cm and 7 cm for the inlet temperatures of 42 °C, 62 °C and 78 °C, and the thermal front movement rates were calculated as 0.050 cm/min, 0.083 cm/min and 0.117 cm/min, respectively. The thermal front movement rate increases with the increasing of the inlet temperature. In addition, the inlet temperature increased 0.86 time (rise from 42 °C to 78 °C), the thermal front movement rate has increased by 1.3 times (rise from 0.050 cm/min to 0.117 cm/min), which indicates that the heat conduction is the main factor controlling the thermal front movement rate of the Selim's thermal model.

(2) The comparison results show that the thermal front movement rates calculated by experiment are much higher than that calculated by the Selim's thermal model under the condition of same basic parameters in NGH reservoir. When the inlet temperature is 42 °C, 62 °C and 78 °C, the thermal front movement rates calculated by experiment are 0.667 cm/min, 0.816 cm/min and 0.833 cm/min (thermal front reached at distances of 42.5 cm, 48 cm and 50 cm in Fig. 5), which are 14.2 times, 9.6 times and 7.1 times higher than that calculated by Selim's thermal model. The significant gap between the Selim's thermal model and the experimental results is mainly because the Selim's thermal model only considers a heat transfer method of heat conduction. Therefore, it is unreasonable that the Selim's thermal model ignores the effect of thermal convection.

Table 2. Basic parameters of NGH reservoir for the Selim's thermal model.

Parameters	Value
Porosity	0.328
Permeability (μm^2)	1.11×10^{-13}
Initial pressure (MPa)	3.4
Initial temperature (°C)	1.0
NGH dissociation temperature (°C)	3.0
Hydrate density (kg m^{-3})	913
Hydrate heat of dissociation (kJ kg^{-1})	400
Gas heat capacity (kJ (kg K)$^{-1}$)	1.238
Thermal diffusivity of hydrate zone (μm^2 s^{-1})	2.615×10^6
Thermal diffusivity of dissociation zone (μm^2 s^{-1})	0.515×10^6
Thermal conductivity of dissociation zone W (m K)$^{-1}$	2.615
Thermal conductivity of hydrate zone W (m K)$^{-1}$	1.288

4 Analysis of theoretical calculation

Heat transfer is an essential part for the hydrate dissociation process since NGH dissociation requires the continuous absorption of heat energy from the periphery. To gain insight into the effects of heat conduction and thermal convection on the thermal front movement rate, the heat flux transferred by heat conduction and thermal convection on the hydrate dissociation process under thermal stimulation is calculated theoretically. The heat flux of convection heat transfer among the hot water and porous medium can be obtained according to the Newton's law of cooling equation (3) [28, 29]. As we know, convection heat transfer includes two heat transfer modes of heat conduction and thermal convection [30, 31]. The heat flux transferred by heat conduction can be calculated according to Fourier's law equation (4) [32]. Thus, the heat flux generated by thermal convection can be given in equation (5)

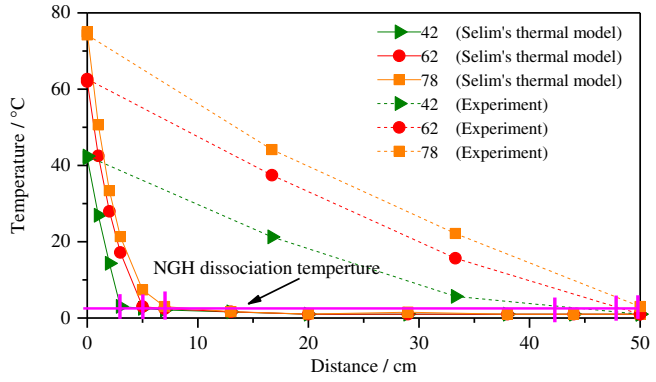

Fig. 5. Distribution of temperature for the Selim's thermal model and experiment.

$$Q = hA(t_f - t_w), \tag{3}$$

$$Q_1 = \frac{\lambda A}{\delta}(t_f - t_w), \tag{4}$$

$$Q_2 = Q - Q_1. \tag{5}$$

The temperature of the hot water is 42 °C, convective heat transfer coefficient was calculated as 43.3 W/(m^2 K) through the empirical formulas [30], the thermal conductivity of NGH is 2.615 W/(m K), and the initial NGH reservoir temperature is 1 °C. According to equations (3)–(5), the total heat flux which is a result of combined action of two heat transfer modes is 1775.3 W, and the heat flux transferred by heat conduction and thermal convection were calculated as 107.2 W and 1668.1 W, respectively. Furthermore, the heat flux transferred by heat conduction only accounts for 6.04% of the total heat flux in the process of NGH thermal stimulation and that by thermal convection accounts for 93.96%, which shows that heat flux transferred by thermal convection is 15.56 times that by heat conduction.

4 Conclusion

In this paper, a NGH thermal stimulation experiment was carried out and its results were compared with the Selim's thermal model. Thermal stimulation experiment results show that the movement rate of thermal front increases with the rise of hot water injection rate, but changes little with the rise of the temperature of the injected hot water. It is indicated that thermal convection is the key factor promoting the thermal front movement and NGH dissociation. The comparison results show that the thermal front movement rates measured in the experiments are about 10 times that by the Selim's thermal model, the reason for which is that the Selim's thermal mathematical model only takes the heat conduction into account. Based on the theoretical calculation, the heat flux transferred by heat conduction only accounts for 6.04% of the total heat transfer in the process of NGH thermal stimulation and that by thermal convection accounts for 93.96%, which shows that heat flux transferred by thermal convection is 15.56 times that by heat conduction. In summary, this paper comes to the conclusion that thermal convection is the main heat transfer mode that controls the movement of thermal front in the process of NGH thermal stimulation, and its influence should never be neglected in those analytical models. To provide a more reliable theoretical basis for NGH reservoir exploitation by thermal stimulation, future analytical models should consider both two kinds of heat transfer modes of the heat conduction and the thermal convection.

Acknowledgments. The work is supported by National Key R&D Program of China (2016YFC0304005), *National Natural Science Foundation of China* (No. 51274227), which are gratefully acknowledged.

References

1 Saikia T., Mahto V. (2018) Temperature augmented visual method for initial screening of hydrate inhibitors, *Oil Gas Sci. Technol. - Rev. IFP Energies nouvelles* **73**, 1.
2 Chen C., Yang L., Jia R., Sun Y.H., Guo W., Chen Y., Li X.T. (2017) Simulation study on the effect of fracturing technology on the production efficiency of natural gas hydrate, *Energies* **10**, 8, 1241.
3 Wang Y., Feng J.C., Li X.S., Zhang Y., Li G. (2015) Analytic modeling and large-scale experimental study of mass and heat transfer during hydrate dissociation in sediment with different dissociation methods, *Energy* **90**, 1931–1948.
4 Hou J., Xia Z.Z., Li S.X., Zhou K., Lu N. (2016) Operation parameter optimization of a gas hydrate reservoir developed by cyclic hot water stimulation with a separated-zone horizontal well based on particle swarm algorithm, *Energy* **96**, 581–591.
5 Liang Y.P., Li X.S., Li B. (2015) Assessment of gas production potential from hydrate reservoir in Qilian Mountain Permafrost using five-spot horizontal well system, *Energies* **8**, 10796–10817.
6 Wang Y., Feng J.C., Li X.S., Zhang Y., Chen Z.Y. (2016) Large scale experimental investigation on influences of reservoir temperature and production pressure on gas production from methane hydrate in sandy sediment, *Energ. Fuel.* **30**, 4, 2760–2770.
7 Lv X.F., Shi B.H., Wang Y., Tang Y.X., Wang L.Y., Gong J. (2014) Experimental study on hydrate induction time of gas-saturated water-in-oil emulsion using a high-pressure flow loop, *Oil Gas Sci. Technol. - Rev. IFP Energies nouvelles* **70**, 6, 1111–1124.
8 Yang Lin, Chen C., Jia R., Sun Y.H., Gou W., Pan D.B., Li X.T., Chen Y. (2018) Influence of reservoir stimulation on marine gas hydrate conversion efficiency in different accumulation conditions, *Energies* **11**, 2, 339.
9 Li S.X., Zheng R.Y., Xu X.H., H, J. (2016) Natural gas hydrate dissociation by hot brine injection, *Petrol. Sci. Technol.* **34**, 5, 422–428.
10 Ding Y.L., Xu C.G., Yu Y.S., Li S.X. (2017) Methane recovery from natural gas hydrate with simulated IGCC syngas, *Energy* **120**, 192–198.
11 Selim M.S., Sloan E.D. (1990) Hydrate dissociation in sediment, *SPE Reserv. Eng.* **5**, 02, 245–251.

12 Tang L.G., Li G., Feng Z.P., Fan S.S. (2006) Mathematic modeling on thermal recovery of natural gas hydrate, *Nat Gas Ind* **26**, 2, 105–107.
13 Li S.X., Jiang X.X., Jiang H.Q., Li Q.Q. (2010) Sensitivity analysis of thermal dissociation of natural gas hydrate, *Oil Drill. Prod. Technol.* **32**, 54–57.
14 Li M.C., Fan S.S., Su Y.L., Justin E., Lu M.J., Zhang L. (2015) Mathematical models of the heat-water dissociation of natural gas hydrates considering a moving Stefan boundary, *Energy* **90**, 202–207.
15 Willhite G.P. (1967) Over-all heat transfer coefficients in steam and hot water injection wells, *J. Pet. Technol.* **19**, 607–615.
16 Ramey H.J.J. (2013) Wellbore heat transmission, *J. Pet. Technol.* **14**, 4, 427–435.
17 Hou J., Sun J.F. (2013) *Thermal recovery technology*, University of Petroleum Press, Dongying, pp. 56–79.
18 Garoosi F., Hoseininejad F., Rashidi M.M. (2016) Numerical study of natural convection heat transfer in a heat exchanger filled with nanofluids, *Energy* **109**, 664–678.
19 Oyama H., Konno Y., Masuda Y. (2009) Dependence of depressurization-induced dissociation of methane hydrate bearing laboratory cores on heat transfer, *Energ. Fuel.* **23**10, 4995–5002.
20 Zhao J.F., Liu D., Yang M.J., Song Y.C. (2014) Analysis of heat transfer effects on gas production from methane hydrate by depressurization, *Int. J. Heat Mass Transfer* **77**, 529–541.
21 Zhao J.F., Wang J.Q., Liu W.G., Song Y.C. (2015) Analysis of heat transfer effects on gas production from methane hydrate by thermal stimulation, *Int. J. Heat Mass Transfer* **87**, 7, 145–150.
22 Hao Y.M., Chen Y.M., Li S.X. (2007) Experimental study on production of natural gas hydrate by thermal stimulation, *J. China Univer. Petrol.* **31**, 4, 60–63.
23 Hao Y.M., Chen X., Li S.X. (2012) Study on the effect of heat injection rate during NGH exploitation by thermal stimulation, *Int. J. Adv. Comput. Technol.* **4**, 21, 550–557.
24 Li S.X., Xu X.X., Zheng R.Y., Chen Y.M., Hou J. (2015) Experimental investigation on dissociation driving force of methane hydrate in porous media, *Fuel* **160**, 117–122.
25 Goel N., Wiggins M., Shah S. (2001) Analytical modeling of gas recovery from in situ hydrates dissociation, *J. Petrol. Sci. Eng.* **29**, 2, 115–127.
26 Li S.X., Cao W., Li J., Gao Y.H. (2014) Experimental study on thermal front movement of natural gas hydrate by injecting hot water, *Geoscience* **28**, 3, 659–662.
27 Chen Y.M., Li S.X., Hao Y.M. (2011) *The theory and technology of natural gas hydrate exploitation*, University of Petroleum Press, Dongying, pp. 246–251.
28 Winterton R.H.S. (1999) Newton's law of cooling, *Contemp. Phys.* **40**, 3, 205–212.
29 Maurone P.A., Shiomos C. (1983) Newton's Law of Cooling with finite reservoirs, *Am. J. Phys.* **51**, 9, 857–859.
30 Whitaker S. (1972) Forced convection heat transfer correlations for flow in pipes, past flat plates, single cylinders, single spheres, and for flow in packed beds and tube bundles, *AICHE J.* **18**, 2, 361–371.
31 Huang S.B. (2014) *Heat transfer theory*, University of Petroleum Press, Dongying, pp. 77–129.
32 Fourier J. (1955) *The analytical theory of heat*, Cambridge University Press, New York.